Nonredundant protective properties of FPR2/ALX in polymicrobial murine sepsis

Thomas Gobbetti[a], Sina M. Coldewey[a,b], Jianmin Chen[a], Simon McArthur[a], Pauline le Faouder[c], Nicolas Cenac[d], Roderick J. Flower[a], Christoph Thiemermann[a], and Mauro Perretti[a,1]

[a]The William Harvey Research Institute, Barts and The London School of Medicine, Queen Mary University of London, London EC1M 6BQ, United Kingdom; [b]Department of Anesthesiology and Intensive Care Medicine, Jena University Hospital, 07743 Jena, Germany; [c]MetaToul Lipidomics Facility, INSERM UMR1048, 31024 Toulouse, France; and [d]INSERM UMR1043, Université Toulouse III Paul-Sabatier, 31024 Toulouse, France

Edited by Fernando Q. Cunha, University of Sao Paulo–Faculty of Medicine of Ribeirao Preto, Ribeiro Preto, Brazil, and accepted by the Editorial Board November 12, 2014 (received for review June 12, 2014)

Sepsis is characterized by overlapping phases of excessive inflammation temporally aligned with an immunosuppressed state, defining a complex clinical scenario that explains the lack of successful therapeutic options. Here we tested whether the formyl-peptide receptor 2/3 (Fpr2/3)—ortholog to human FPR2/ALX (receptor for lipoxin A4)—exerted regulatory and organ-protective functions in experimental sepsis. Coecal ligature and puncture was performed to obtain nonlethal polymicrobial sepsis, with animals receiving antibiotics and analgesics. Clinical symptoms, temperature, and heart function were monitored up to 24 h. Peritoneal lavage and plasma samples were analyzed for proinflammatory and proresolving markers of inflammation and organ dysfunction. Compared with wild-type mice, Fpr2/3$^{-/-}$ animals exhibited exacerbation of disease severity, including hypothermia and cardiac dysfunction. This scenario was paralleled by higher levels of cytokines [CXCL1 (CXC receptor ligand 1), CCL2 (CC receptor ligand 2), and TNFα] as quantified in cell-free biological fluids. Reduced monocyte recruitment in peritoneal lavages of Fpr2/3$^{-/-}$ animals was reflected by a higher granulocyte/monocyte ratio. Monitoring Fpr2/3$^{-/-}$ gene promoter activity with a GFP proxy marker revealed an over threefold increase in granulocyte and monocyte signals at 24 h post-coecal ligature and puncture, a response mediated by TNFα. Treatment with a receptor peptido-agonist conferred protection against myocardial dysfunction in wild-type, but not Fpr2/3$^{-/-}$, animals. Therefore, coordinated physio-pharmacological analyses indicate nonredundant modulatory functions for Fpr2/3 in experimental sepsis, opening new opportunities to manipulate the host response for therapeutic development.

resolution of inflammation | therapeutic innovation | annexin peptide | ALX | cardiac dysfunction

Sepsis is a clinical syndrome expression of the host reaction to pathogen invasion, as a consequence of either direct dissemination into the bloodstream or postsurgical trauma and gut ischemia/reperfusion-mediated pathogen translocation. The complexity of sepsis is due to multiple local and systemic immune responses that involve release of soluble mediators such as cytokines, bioactive lipid mediators, and cell stress markers, leading to multiple organ failure and ultimately death (1). Originally believed to result exclusively from an overzealous inflammatory response (e.g., cytokine storm), the lack of efficacy of anticytokine therapy in several clinical trials demonstrated that the pathogenesis of sepsis is complex. Notwithstanding the difficulty in clinical cases to establish the beginning of the infection (and the temporal recruitment of failing organs), it is now appreciated that the systemic inflammatory response syndrome (SIRS) can overlap with a compensatory anti-inflammatory response syndrome (CARS) (2). Immunosuppression associated with CARS may explain the failure of classical anti-inflammatory strategies in patients (3, 4).

The acute inflammatory reaction against pathogens is in many cases successful, leading to healing and recovery of biological function. To achieve this end point, specific mediators and pathways of endogenous protection must be engaged by the host to promote what is now referred to as "resolution of inflammation" (5). Proresolving mediators share a set of properties that are emerging as paradigmatic (6); these include modulation of immune cell recruitment [inhibition of polymorphonuclear (PMN) migration and promotion of monocyte influx], augmentation of phagocytosis (leading to bacteria containment), promotion of apoptosis and efferocytosis, and eventually tissue/organ repair with restoration of physiological function (6, 7). It is perhaps for these organic and multifactorial biological actions that proresolving mediators like the protein annexin A1 (AnxA1) and the bioactive lipids lipoxin A_4 (LXA_4) and resolvin D_2 exert protection in models of experimental sepsis (8–10). Of relevance, the receptor target for AnxA1 and LXA_4 is a G protein-coupled receptor that belongs to the formyl-peptide receptor (FPR) family, termed FPR2/ALX. To establish the validity of FPR2/ALX for the development of innovative therapeutic approaches, proof-of-concept data within loss-of-function settings should be established.

In the mouse, the human *FPR2/ALX* gene corresponds to two genes, termed *Fpr2* and *Fpr3*, which share the first of the two exons (11). LXA_4 and AnxA1 are largely inactive in a transgenic mouse that lacks both murine genes (12) as shown in models of acute inflammation and ischemia-reperfusion injury (12–15). Herein we establish the patho-pharmacology of Fpr2/3 in experimental polymicrobial sepsis as a way to validate the human

Significance

Sepsis defines a syndrome with poor clinical management characterized by overlapping phases of excessive inflammation temporally aligned with an immunosuppressed state. We define an endogenous pathway centered on formyl-peptide receptor 2/3 (Fpr2/3)—ortholog to human FPR2/ALX (receptor for lipoxin A4)—that protects the host against polymicrobial sepsis. Using null mice and proof-of-concept experiments with a peptide–agonist, we demonstrate how engagement of Fpr2/3 is crucial to enact nonredundant functions that span from control of cell recruitment and phagocytosis, modulation of soluble mediator generation, to containment of bacteremia, thus preventing spreading to vital organs and opening new opportunities to manipulate the host response in sepsis.

Author contributions: T.G., R.J.F., C.T., and M.P. designed research; T.G., S.M.C., J.C., S.M., P.I.F., and N.C. performed research; T.G., S.M.C., J.C., S.M., P.I.F., and N.C. analyzed data; and T.G. and M.P. wrote the paper.

The authors declare no conflict of interest.

This article is a PNAS Direct Submission. F.Q.C. is a guest editor invited by the Editorial Board.

Freely available online through the PNAS open access option.

[1]To whom correspondence should be addressed. Email: m.perretti@qmul.ac.uk.

This article contains supporting information online at www.pnas.org/lookup/suppl/doi:10.1073/pnas.1410938111/-/DCSupplemental.

ortholog as a genuine receptor target for innovative treatments in sepsis.

Results

Fpr2/3 Deficiency Aggravates the Host Response to Microbial Sepsis. Induction of polymicrobial sepsis yielded worse clinical scores for Fpr2/3$^{-/-}$ mice compared with WT animals: At 24 h post-coecal ligature and puncture (CLP), WT mice developed moderate sepsis (82%; score, ≤3), whereas 73% of Fpr2/3$^{-/-}$ mice recorded a score >3, indicating severe sepsis (Fig. 1*A*). Rectal temperature 12 h post-CLP was decreased in both genotypes, however Fpr2/3$^{-/-}$ mice displayed prolonged hypothermia (Fig. 1*B*).

Analyses of peritoneal exudates by flow cytometry (Fig. 1*C*) demonstrated increased peritoneal leukocyte recruitment 12 h post-CLP in Fpr2/3$^{-/-}$ mice (Fig. S1*A*), largely due to increased Ly6G^{+} recruitment (Fig. 1*D*). At 24 h post-CLP, neutrophil numbers did not differ between genotypes, but the total number of F4/80^{low} monocytes was lower in Fpr2/3$^{-/-}$ mice (Fig. 1*E*). This paucity of monocyte numbers was confirmed by immunohistochemistry (Iba1^{+ve} cells; Fig. S1*B*) and yielded a marked increase in neutrophil/monocyte ratio in Fpr2/3$^{-/-}$ mice (Fig. 1*E*, *Inset*). Analysis of T-lymphocyte and B-lymphocyte numbers revealed no difference between genotypes (Fig. S1 *C* and *D*).

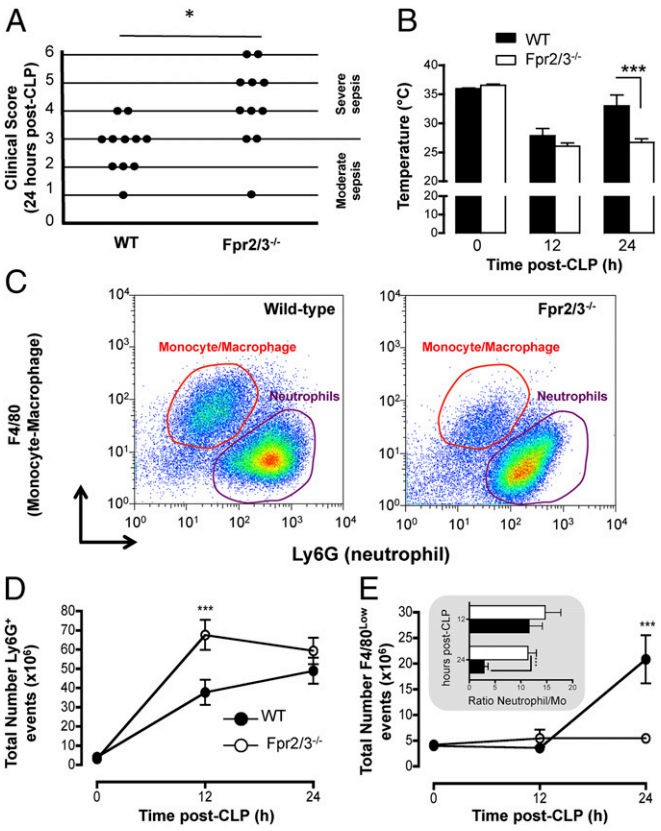

Fig. 1. Fpr2/3 deficiency aggravates response to microbial sepsis. WT and Fpr2/3$^{-/-}$ mice were subjected to CLP at time 0. (*A*) At 24 h post-CLP, mice were scored for the presence or absence of six different macroscopic signs of sepsis (*SI Methods*). A clinical score >3 is considered as severe sepsis. Data are from 11 mice; *$P < 0.05$ (Fisher's exact test). (*B*) Temporal changes in rectal temperature post-CLP in WT and Fpr2/3$^{-/-}$ animals. (*C*) Scattergrams illustrating neutrophil (identified as Ly6G+F4/80–) and monocyte–macrophage (identified as Ly6G–F4/80+) positive events in peritoneal lavages from WT and Fpr2/3$^{-/-}$ mice at 24 h post-CLP. (*D* and *E*) Cumulative data for peritoneal Ly6G+ and F4/80+ cells. (*Inset*) Ratios of neutrophils/monocytes. Data are mean ± SEM of six mice per genotype. ***$P < 0.001$ versus respective WT value (two-way ANOVA, post hoc Tukey test).

Thus, Fpr2/3 deficiency aggravates the host response to microbial sepsis and impairs the timely resolution of peritoneal inflammation. The augmented Ly6G^{+} neutrophil recruitment observed following CLP in Fpr2/3$^{-/-}$ mice was not indicative of indiscriminate higher extents of cell trafficking, as leukotriene B_4, KC [keratinocyte chemokine, also termed CXCL1 (CXC receptor ligand 1)], and TNFα evoked similar recruitment in the two genotypes (Fig. S2).

Soluble Mediator Generation in Fpr2/3$^{-/-}$ Mice. Assessment of exudate cytokine levels revealed selected alterations in Fpr2/3$^{-/-}$ mice with higher levels of KC, MCP-1 [monocyte chemoattractant protein 1, also termed CCL2 (CC receptor ligand 2)], and IL-6. TNFα, IFNγ, IL-10, and IL-17α levels incremented to a similar degree at 12 h, yet they remained elevated at 24 h post-CLP in Fpr2/3$^{-/-}$ animals (Fig. S3). In the plasma, specific cytokines were detected, with increased levels of KC, IL-6, TNFα, and IFNγ 24 h post-CLP in Fpr2/3$^{-/-}$ mice (Fig. S4). Liquid chromatography–MS/MS (LC–MS/MS) spectroscopy allowed determination of multiple bioactive lipids with significantly augmented levels of PGE_2 and 6-keto-$PGF_{1\alpha}$ in peritoneal exudates of Fpr2/3$^{-/-}$ mice (Table S1).

We then analyzed the presence of the Fpr2/3 agonists AnxA1 and LXA_4. At the time points under observation, peritoneal levels of AnxA1 increased more than fourfold, over sham, with no difference between genotypes. LXA_4 levels were markedly increased in Fpr2/3$^{-/-}$ mice 24 h post-CLP, whereas levels were much lower in WT animals (Fig. S5).

Fpr2/3 Absence Impairs Bacterial Clearance. As a worse outcome of sepsis is associated with bacteremia (16) and Fpr2/3 agonists promote bacterial phagocytosis in vitro (17), we investigated whether Fpr2/3$^{-/-}$ mice displayed altered bacterial clearance in vivo. Fig. 2 shows that Fpr2/3$^{-/-}$ mice exhibited higher peritoneal bacteria content following CLP as quantified by flow cytometry (Fig. 2 *A* and *B* and Fig. S6*A*), a result confirmed also through peritoneal bacterial colony counts (Fig. S6*B*). Blood bacteria counts were also elevated in Fpr2/3$^{-/-}$ mice (Fig. S6*C*).

As neutrophils were the principal cell type present in the inflammatory exudates of Fpr2/3$^{-/-}$ mice post-CLP, we investigated whether the phagocytic ability of this cell type was compromised. Exudate neutrophils from Fpr2/3$^{-/-}$ mice phagocytosed much less *Escherichia coli* than WT cells (Fig. 2 *C* and *D*). Addition of AnxA1 to WT neutrophils incremented both the proportion of cells with internalized bacteria (Fig. 2*E*) and their median fluorescence intensity (a sign for higher engulfment per cell; Fig. 2*F*), effects absent in neutrophils lacking Fpr2/3. Efficiency of bacteria killing was investigated next. Following 2 h of incubation, WT exudate neutrophils (*SI Methods*) killed ∼13% of phagocytized bacteria, whereas Fpr2/3$^{-/-}$ cells displayed minimal bactericidal capability (Fig. 2*G*). Collectively, these data demonstrate fundamental properties for host Fpr2/3 to manage peritoneal bacteria infection.

Fpr2/3 Gene Modulation in Immune Cells During Sepsis. Fpr2/3$^{-/-}$ mice bear an in-frame GFP reporter construct (12). Following CLP, a ∼threefold increase in GFP signal was measured in F4/80^{+ve} monocytes, with >twofold in Ly6G^{+} neutrophils (Fig. 3*A*). To investigate the activating role of soluble mediators, Fpr2/3$^{-/-}$ peritoneal macrophages were incubated with peritoneal lavages from CLP WT or Fpr2/3$^{-/-}$ animals. At 24 h, increased GFP expression was measured, whereas lavages from sham-operated animals were inactive (Fig. S7*A*). This outcome was irrespective of genotype.

Next, macrophages were incubated with single proinflammatory cytokines, yet *Fpr2/3* gene activation was solely induced by TNFα, as shown by (*i*) increased GFP fluorescence intensity (using Fpr2/3$^{-/-}$ cells; Fig. 3*B*) and (*ii*) elevated Fpr2/3 mRNA message in WT but not TNFα type I receptor null macrophages (Fig. S7*B*). Similar results could be replicated in mouse

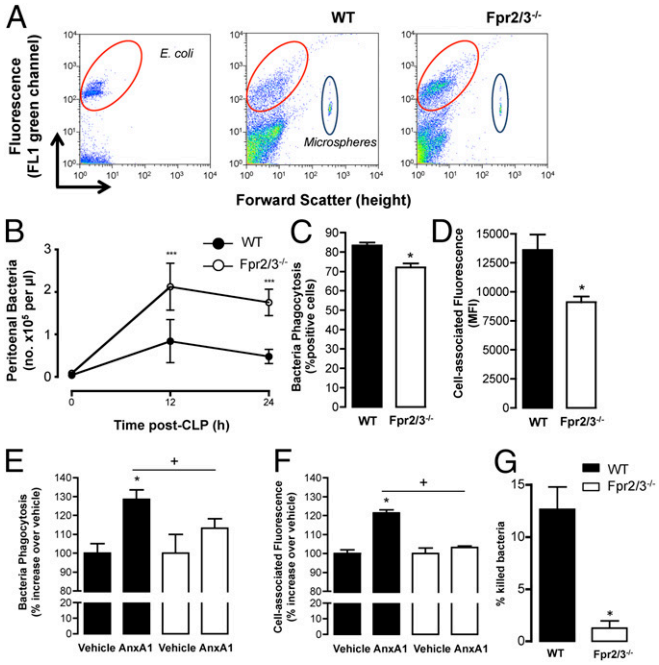

Fig. 2. Inadequate bacterial clearance in the absence of Fpr2/3. WT and Fpr2/3$^{-/-}$ mice were subjected to CLP at time 0. (*A*) Representative flow cytometry scattergrams illustrating bacteria (SYTO BC bacteria dye) positive events in *E. coli* suspension (*Left*) as well as 24 h post-CLP peritoneal exudates from WT and Fpr2/3$^{-/-}$ mice. The density of bacteria in the experimental samples was determined from the ratio of bacterial to microsphere signals. (*B*) Bacteria levels in peritoneal lavages from WT and Fpr2/3$^{-/-}$ mice. Data are mean ± SEM of six mice. ***$P < 0.001$ versus correspondent WT value (two-way ANOVA, post hoc Tukey test). (*C* and *D*) In vitro bacteria phagocytosis by zymosan-elicited neutrophils following incubation with pHrodo Red *E. coli* BioParticles for 90 min at 37 °C. (*C*) Bacteria phagocytosis represented as percentage of positive cells. (*D*) Cell-associated fluorescence measured as median fluorescence intensity (MFI) units. Data are mean ± SEM of six mice. *$P < 0.05$ versus correspondent WT value (Student *t* test). (*E* and *F*) Effect of AnxA1 (10 nM; 4 h at 37 °C) on neutrophil phagocytosis of pHrodo Red *E. coli* BioParticles and cellular MFI intensity. Data are mean ± SEM of 3–4 mice per group. *$P < 0.05$ versus vehicle; $^{+}P < 0.05$ versus correspondent WT value (two-way ANOVA, post hoc Tukey test). (*G*) Zymosan-induced peritoneal cells were incubated with opsonized *E. coli* for 2 h and bactericidal activity determined using a gentamicin survival assay. Data are mean ± SEM of three mice. *$P < 0.05$ versus correspondent WT value (Student *t* test).

bone marrow-derived neutrophils (Fig. S7*C*). TNFα treatment of human primary blood monocytes enhanced cell surface FPR2/ALX receptor expression (Fig. S7*D*).

Cardiac Dysfunction Following Polymicrobial Sepsis Is Exacerbated by Fpr2/3 Deficiency. The principal cause of mortality in sepsis is organ failure, with heart, liver, and kidney being among the most commonly affected organs (16). In our settings, CLP had no effect on plasma creatinine and urea levels (indicative of renal dysfunction) in WT animals, except for a transient increase in urea levels significant at 12 h post-CLP (Fig. S8 *A* and *B*). However, compared with WT, CLP Fpr2/3$^{-/-}$ mice demonstrated a significant increase in plasma urea (12 h and 24 h post-CLP) and creatinine (24 h time point), indications for development of acute kidney injury (Fig. S8 *A* and *B*). For liver dysfunction, both genotypes exhibited increased levels of plasma alanine aminotransferase and aspartate aminotransferase markers following CLP, however alanine aminotransferase levels augmented to a significantly greater degree after 12 h in Fpr2/3$^{-/-}$ mice (Fig. S8 *C* and *D*). There was some evidence for higher granulocyte recruitment in Fpr2/3$^{-/-}$ organs, measured as myeloperoxidase (MPO) activity, albeit modest, with an evident difference in null mouse kidney at 24 h post-CLP (Fig. S8 *E* and *F*).

Left ventricular functionality was assessed in vivo using echocardiography. Fig. 4*A* presents typical M-mode echocardiograms of sham and CLP mice. Sham mice demonstrated no significant differences in percentage ejection fraction, fractional shortening, or fractional area change (Fig. 4 *B*–*D*) between the two genotypes. WT CLP mice demonstrated a significant reduction in all three parameters, indicative of impaired systolic contractility (visually shown in Fig. 4*A*). Lack of Fpr2/3 exacerbated cardiac dysfunction with significant reductions in ejection fraction (–45%), fractional shortening (–37%), and fractional area of change (–59%) (Fig. 4 *B*–*D*). No significant differences were apparent between the two genotypes in terms of heart rate (Fig. 4*E*) or granulocyte recruitment (assessed by MPO activity; Fig. 4*F*). Despite the compromised cardiac function, WT animals did not show increased plasma levels of Troponin-I at 24 h post-CLP, however these were elevated in Fpr2/3$^{-/-}$ mice, indicative of unabated cardiac dysfunction (Fig. 4*F*). Finally, both Fpr2 and Fpr1 mRNA expression was increased in WT heart tissue samples 24 h post-CLP (Fig. 4*G*).

Together, these data demonstrate that endogenous activation of Fpr2/3 plays a major role in dampening dysfunction in distinct organs during polymicrobial sepsis, with a particular efficacy in preserving cardiac function.

Fpr2/3 Agonism Protects Against Myocardial Dysfunction. Finally, we investigated the therapeutic potential of a stable AnxA1-based FPR2/ALX agonist (18). Administration of CR-Ac$_{2–50}$ (3 μg or 550 pmol per mouse) improved cardiac function: These protective actions were not observed in mice lacking Fpr2/3 (Fig. 5 *A*–*C*). Treatment with the peptide did not alter markers of liver dysfunction (Fig. S9 *A* and *B*), whereas an effect on kidney markers was evident at 24 h post-CLP. Peptide CR-Ac$_{2–50}$ improved the clinical status of WT animals, again with no efficacy in Fpr2/3$^{-/-}$ animals (Fig. S9*C*). Administration of peptide CR-Ac$_{2–50}$ decreased the total number of both neutrophils and monocytes recruited 24 h post-CLP in WT mice (Fig. S8 *D*–*F*). A tendency in the reduction of peritoneal bacteremia was seen post–CR-Ac$_{2–50}$ administration (Fig. S9*G*). Assessment of exudate cytokines demonstrated that although IL-6, IL-1α, IFNγ, IL-17α, KC, and MCP1 content was not altered (values comparable to vehicle group), CR-Ac$_{2–50}$ decreased (~35%) TNFα levels in WT, but not Fpr2/3$^{-/-}$,

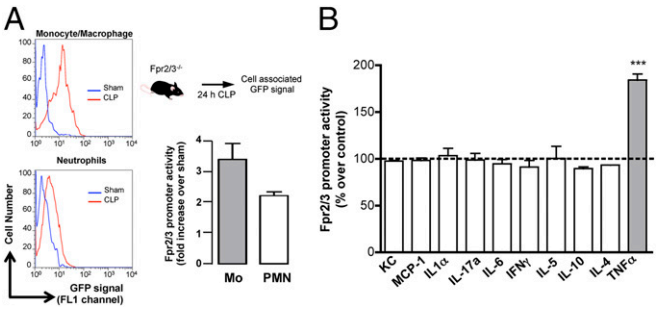

Fig. 3. Modulation of Fpr2/3 gene expression in immune cells during polymicrobial sepsis. (*A*) Fpr2/3$^{-/-}$ mice, bearing an in-frame GFP reporter construct, were subjected to CLP at time 0 and exudates collected at the 24 h time point. (*Left*) Representative histograms showing GFP fluorescence as quantified by flow cytometry in monocytes (Mo) and neutrophils (PMN) from sham (blue) or CLP (red) exudates. (*Right*) Cumulative data showing increment over sham in cell-associated GFP. Mean ± SEM, six mice. (*B*) Biogel-elicited macrophages from Fpr2/3$^{-/-}$ mice were incubated with the indicated cytokines (all at 50 ng/mL) for 24 h at 37 °C before assessment of GFP fluorescence by flow cytometry. Data are mean ± SEM of 3–4 distinct cell preparations. ***$P < 0.001$ versus control (one-way ANOVA, post hoc Dunnet test).

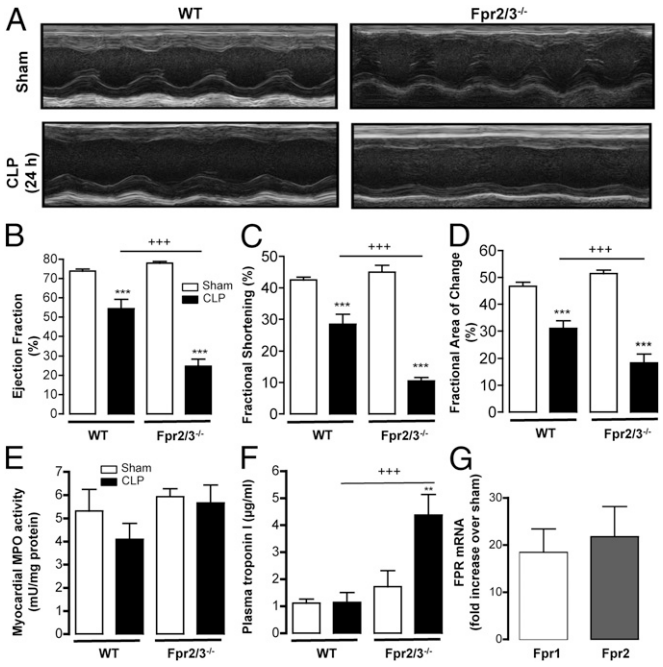

Fig. 4. Cardiac dysfunction following polymicrobial sepsis is exacerbated by Fpr2/3 deficiency. WT and Fpr2/3$^{-/-}$ mice were subjected to CLP at time 0 before analysis of cardiac function at the 24 h time point by echocardiography. (*A*) Representative M-mode echocardiograms 24 h post-CLP or sham from WT or Fpr2/3$^{-/-}$ mice. (*B*) Cumulative data for percentage ejection fraction measured as percent of the total amount of blood ejected in the left ventricle with each heartbeat. (*C*) Cumulative data for fractional shortening measured as percent of left ventricle internal diameters between the diastolic and systolic phases. (*D*) Cumulative data for fractional area of change measured as percent change in left ventricular cross-sectional area between diastole and systole. (*E*) Myocardial MPO activity 24 h post-CLP or sham samples from WT or Fpr2/3$^{-/-}$ mice. (*F*) Plasma troponin I levels 24 h post-CLP or sham samples from WT or Fpr2/3$^{-/-}$ mice. (*B–F*) Mean ± SEM of six mice. ***$P < 0.001$ versus corresponding sham value; $^{+++}P < 0.001$ between genotypes (two-way ANOVA, post hoc Tukey test). (*G*) WT myocardial Fpr1 and Fpr2 mRNA quantification by real-time PCR. Data are expressed as fold CLP increase over sham (mean ± SEM of six mice).

mice (Fig. S9*H*). Plasma levels of TNFα and IL-6 levels were also reduced (Fig. S9 *I* and *J*).

Together, these data demonstrate that exogenous activation of Fpr2/3 affords marked improvement of cardiac dysfunction following sepsis, possibly consequent to modulation of the inflammatory response both locally and in the circulation.

Discussion

We characterize here a nonredundant endogenous pathway that protects the host against disseminated polymicrobial sepsis. Engagement of Fpr2/3 (mouse ortholog of human FPR2/ALX) is crucial to enact nonredundant functions that span from cell recruitment to phagocytosis, from control of soluble mediator generation to containment of inflammation within the site, thus preventing spreading to vital organs. The augmented impaired function detected in the kidney and heart is indicative of fundamental protective properties evoked by FPR2/3, which could be harnessed by the exogenous administration of peptide CR-Anx$_{2–50}$.

The consensus definition of sepsis as a SIRS that occurs during infection (19) propelled the trialing of different anti-inflammatory approaches ranging from corticosteroids (20) to neutralizing anti-endotoxin strategies (21) and from TNFα (3, 22) to IL-1 receptor antagonist (23). Unfortunately, none of these treatments resulted in effectively reducing mortality; rather, in some cases, they were detrimental (22). Therefore, sepsis remains a major clinical challenge, and the need for new treatments is urgent.

CLP, the gold standard model of sepsis, produces a polymicrobial infection with ensuing immune, hemodynamic, and biochemical responses that replicate those observed in patients with sepsis (24). Older patients are more frequently affected by sepsis, and the treatment at intensive care units is, except for early administration of antibiotics, mostly of a supportive nature, including vasopressor therapy and fluid replenishment (25). In this study, we simulated these conditions by performing CLP in 8-mo-old mice treated with a large spectrum of antibiotic and fluids (26, 27). Fpr2/3$^{-/-}$ mice developed longer lasting macroscopic signs of severe sepsis, as evident from 24 h of hypothermia, than WT animals.

The homeostatic functions of proresolving and tissue-protective pathways are now emerging in several immune contexts, including arthritis, colitis, periodontal pathologies (5), and ischemia/reperfusion damage (13). The complex biological functions affected by Fpr2/3 afforded efficacy against polymicrobial sepsis downstream of positive modulation of multiple life-saving processes through a single receptor determinant. Indeed, the appreciation that sepsis is not just SIRS but rather a complex clinical setting with an overlapping CARS indicates that innovative approaches must be proposed.

There is experimental evidence that endogenous agonists of Fpr2/3 are protective in experimental sepsis. The omega-6 derivative LXA$_4$, administered to CLP rats increases survival rates and attenuates tissue injury (9). The omega-3 derivative resolvin D$_1$ improves the outcome of sepsis (28). Work from our group has identified marked *Anxa1* gene activation in experimental endotoxaemia, together with a higher toxic response in AnxA1$^{-/-}$ mice, a phenotype rescued by exogenous application of the protein (8). From a therapeutic perspective, a recent study conducted with peptide WKYMVm, a panagonist at FPRs, described the control of severe sepsis after microbial infection (29). Albeit interesting, this study does not provide target validation to the properties of FPR2/ALX agonists and focuses solely on the host immune response rather than complementing it with organ functionality. These pharmacological studies indicate a role for Fpr2/3, but the mechanism(s) it might control in the contest of sepsis remained unexplored.

The Fpr2/3 agonists AnxA1 and LXA$_4$ could be detected in peritoneal infected exudates with an interesting "overshooting" of the latter in Fpr2/3$^{-/-}$ mice, likely indicative of a "frustrated" compensatory loop to dampen the exacerbated inflammatory response. This would also suggest that LXA$_4$ is the pivotal agonist in these settings or, rather, that a temporal distinction for agonist generation exists, when one compares profiles of AnxA1 and LXA$_4$ levels in WT mice. Following detection of endogenous agonists, we noted that a variety of host responses were altered when the Fpr2/3 axis was not engaged, pointing again to nonredundant multiple

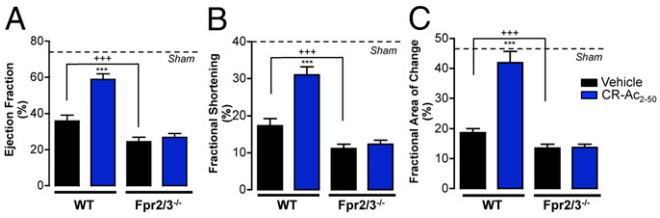

Fig. 5. Fpr2/3 agonism modulates organ injury in polymicrobial sepsis. WT and Fpr2/3$^{-/-}$ mice were subjected to CLP at time 0 and treated with peptide CR-Ac$_{2–50}$ 1 h and 9 h postsurgery (90 μg/kg i.p.), or with vehicle (100 μL i.p.), before being sacrificed at 24 h post-CLP. (*A–C*) Assessment of myocardial dysfunction by echocardiography; mean ± SEM of six mice per group. *$P < 0.05$, **$P < 0.01$, ***$P < 0.001$ versus correspondent vehicle value; $^{+++}P < 0.001$ between genotypes (two-way ANOVA, post hoc Tukey test).

regulatory functions. Thus, selected changes in cytokine and chemokine levels were associated with augmented bioactive lipid generations. Of interest, major differences were measured for KC (CXCL1), MCP-1 (CCL2), and IL-6. High MCP-1 levels were not married by an efficient monocyte influx (quite the opposite), indicating the requirement for other pathways to bring in monocytes, a crucial process for the in situ differentiation into phagocytozing macrophages that regulate resolution (30). It is plausible that CCR2 independent pathways might be altered. Relevantly, LXA_4 can promote nonphlogistic monocyte migration (31), and the same occurs for another Fpr2/3 ligand, the cathelicidin LL-37 (32).

The poor recruitment of monocytes observed in Fpr2/3$^{-/-}$ animals is functionally linked to a lower number of macrophages, higher neutrophil/monocyte–macrophage ratios, and inadequate bacterial removal. Congruently, clearance of bacteria from the peritoneal cavity was markedly reduced in Fpr2/3$^{-/-}$ mice, possibly enacting a vicious circle leading to potentiation of inflammation and delayed resolution, as evident from the higher cfu formation in Fpr2/3$^{-/-}$ peritoneal fluids. Bacteria counts were also elevated in the circulation. Analyses of cell behavior indicated, besides defective recruitment, a direct impairment of phagocyte functions in Fpr2/3$^{-/-}$ neutrophils. Although not in these settings, studies have demonstrated the importance of AnxA1, LXA_4, and more recently resolvin D_1 in promoting particle phagocytosis and efferocytosis by immune cells (17, 33, 34) together with ineffectiveness in cells lacking Fpr2/3 (35).

The ultimate cause of death in patients with sepsis is multiple organ failure. Absence of Fpr2/3 was associated with major changes in distant organ injury, with a particular effect upon heart and kidney. An exacerbated myocardial dysfunction occurred in the transgenic, as reflected by a marked profound decrease in ejection fraction, fractional shortening, or fractional area. Myocardial dysfunction frequently accompanies severe sepsis (36), yet the distinctive feature of myocardial dysfunction does not appear to be the hypoperfusion of the heart but rather the release of circulating depressant factors, including cytokines like TNFα (37). Indeed, high levels of cytokines quantified in Fpr2/3$^{-/-}$ mice could underlie organ dysfunction: There are indications that unabated circulating cytokines are predictive of early mortality in sepsis (38). Some of them, like TNFα and IL-1β, can exert a direct effect through increased expression of inducible NO synthase (39, 40). In any case, the augmented myocardial injury determined by Fpr2/3 absence was functional, as evident with poor systolic pressure and pulse.

Whereas liver and lungs were mildly affected in the CLP model, with little or no difference between the two genotypes, different responses were quantified for the kidney parameters. The kidney is relatively resistant, and indeed markers of injury were not elevated in WT mice subjected to our protocol of sepsis. In contrast, elevated urea and creatinine plasma levels were measured in Fpr2/3$^{-/-}$ mice. Kidney MPO activity, an index of granulocyte tissue recruitment, was increased in the null animal, prompting speculation that—at least in part—unchecked inflammation could be the cause of acute kidney injury experienced by Fpr2/3$^{-/-}$ mice. Cellular infiltrates, particularly neutrophils, damage tissue directly by realizing lysosomal enzymes and superoxide-derived radicals (41). It is also plausible that the hypotension/vasodilatation derived from impaired cardiac function could at least contribute to kidney damage.

Two sets of data merit further discussion. The first one entails the pivotal role played by TNFα, but not other cytokines tested, in activating the Fpr2/3 gene promoter, as demonstrated using a combination of reporter assays ex vivo and in vitro, with analyses in mouse and human cells. The appreciation that proinflammatory mediators set in motion the resolution and protective phase of inflammation is emerging (42), yet our data solidly show this link and identify TNFα as the culprit, acting through the type I receptor. This set of data extends previous in vitro observations in synovial fibroblasts (43) and mouse microglial cells (44). It could be speculated that failure of anti-TNFα strategies in sepsis may, at least in part, be due to inadequate induction of a protective pathway in the host, including AnxA1, the agonist (8), and its receptor Fpr2/3 (this study).

The second comment relates to the pharmacological experiments with CR-$Ac_{2–50}$. Therapeutic delivery of this peptide, highly selectivity for human FPR2/ALX (IC_{50}, ~10 nM) over FPR1 (18), afforded marked protection. It is relevant here that CR-$Ac_{2–50}$ inhibited neutrophil trafficking while enhancing macrophage efferocytosis in sterile inflammation (18), possessing therefore a few of the necessary properties, as discussed above, to elicit host protection. Control of the immune response by CR-$Ac_{2–50}$ was complemented by a significant attenuation of the impairment in systolic contractility. This effect can reflect an indirect protection through reduced inflammation but also could be the consequence of a direct protective action on the myocardium, preserving its contractile function (45, 46). None of these biological properties were retained in Fpr2/3$^{-/-}$ mice. The documented increase in myocardial mRNA for Fpr1 and Fpr2 can be explored in future investigations. These data complement recent studies conducted with panagonists of formyl peptide receptors (28, 29).

In conclusion, we describe nonredundant properties of endogenous Fpr2/3, the receptor determinant for agonists of the resolution of inflammation process, in a model of polymicrobial sepsis. This nonredundant role stems from multiple biological functions controlled by this master receptor, which is able to set in motion an integrated battery of host-protective effects operative both at the site of infection and in distant vital organs (Fig. 6). Therapeutic innovation in the management of sepsis can derive from the development of selective Fpr2/3 (and FPR2/ALX in man) agonists, and this could include small molecules, peptidomimetics, as well as bioactive lipid derivatives (47).

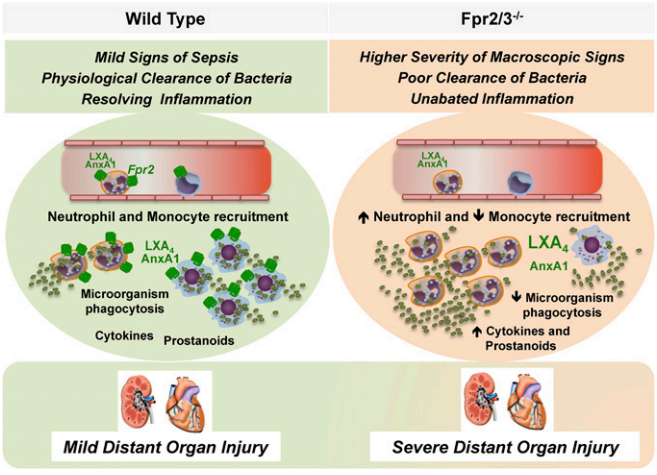

Fig. 6. Loss of host control on polymicrobial sepsis in the absence of Fpr2/3. The control exerted by endogenous engagement of FPR2/ALX (mimicked here by its orthologs Fpr2/3) is dual: regulation for an optimal local reaction with proper dealing by host immune cells with the bacteria load, and modulation of circulating mediators and distant organ functionality (heart and kidney).

Methods

SI Methods provides an extended version of the experimental procedures.

Polymicrobial Sepsis. CLP was performed in 8-mo-old male C57BL/6 or *Fpr2/3*$^{GFP/GFP}$ (thereafter referred to as Fpr2/3$^{-/-}$) mice, bearing a knocked-in gene for green fluorescent protein (12), using a protocol that mimics clinical management in intensive care units including fluid resuscitation, antibiotic therapy, and analgesia

after surgery (27). In some experiments, mice were treated with peptide CR-AnxA1$_{2–50}$. A clinical score for monitoring the health of experimental mice was used. Animals were killed 12 or 24 h later. All animal experiments were approved by the local Animal Use and Care Committee in accordance with the United Kingdom Animals (Scientific Procedures) Act of 1986. Human cells were prepared according to an approved protocol (East London & the City Local Research Ethics Committee; no. 06/Q605/40; P/00/029).

Assessment of Cardiac Function in Vivo. Cardiac function was assessed in mice by echocardiography (48).

Bacteria Counting. Accurate enumeration of bacteria in peritoneal lavages was performed by flow cytometry using the SYTO BC bacteria counting kit. Blood and peritoneal bacteria loads were also determined by growth on a tryptic soy agar plate, as reported (10).

Peritoneal Lavage Lipid Quantification. Quantification of 6kPGF$_{1\alpha}$, TXB$_2$, PGE$_2$, LxA$_4$, LTB$_4$, and PGD$_2$ in peritoneal lavages was achieved by LC–MS/MS measurements as described (49).

Neutrophil Phagocytosis and Killing Assay. Exudate neutrophils (50) were labeled with anti-Ly6G, and phagocytosis of pH-sensitive Phrodo *E. coli* bioparticles was measured by flow cytometry. Neutrophil bactericidal activity was measured following incubation with opsonized *E. coli*.

ACKNOWLEDGMENTS. We thank Drs. Gaston-Massuet and Allan for TNFα type I receptor null animals. Funding was provided by Welcome Trust Programme Grant 086867/Z/08/Z. S.M.C. was funded by a Fellowship of the German Research Foundation (CO 912/1-2). This work forms part of the research themes contributing to the translational research portfolio of Barts and The London National Institute for Health Research Cardiovascular Biomedical Research Unit.

1. Aziz M, Jacob A, Yang WL, Matsuda A, Wang P (2013) Current trends in inflammatory and immunomodulatory mediators in sepsis. *J Leukoc Biol* 93(3):329–342.
2. Hotchkiss RS, Coopersmith CM, McDunn JE, Ferguson TA (2009) The sepsis seesaw: Tilting toward immunosuppression. *Nat Med* 15(5):496–497.
3. Abraham E, et al. (1995) Efficacy and safety of monoclonal antibody to human tumor necrosis factor alpha in patients with sepsis syndrome. A randomized, controlled, double-blind, multicenter clinical trial. TNF-alpha MAb Sepsis Study Group. *JAMA* 273(12):934–941.
4. Deans KJ, Haley M, Natanson C, Eichacker PQ, Minneci PC (2005) Novel therapies for sepsis: A review. *J Trauma* 58(4):867–874.
5. Serhan CN (2011) The resolution of inflammation: The devil in the flask and in the details. *FASEB J* 25(5):1441–1448.
6. Ortega-Gómez A, Perretti M, Soehnlein O (2013) Resolution of inflammation: An integrated view. *EMBO Mol Med* 5(5):661–674.
7. Serhan CN (2010) Novel lipid mediators and resolution mechanisms in acute inflammation: To resolve or not? *Am J Pathol* 177(4):1576–1591.
8. Damazo AS, et al. (2005) Critical protective role for annexin 1 gene expression in the endotoxemic murine microcirculation. *Am J Pathol* 166(6):1607–1617.
9. Walker J, et al. (2011) Lipoxin a$_4$ increases survival by decreasing systemic inflammation and bacterial load in sepsis. *Shock* 36(4):410–416.
10. Spite M, et al. (2009) Resolvin D2 is a potent regulator of leukocytes and controls microbial sepsis. *Nature* 461(7268):1287–1291.
11. Ye RD, et al. (2009) International Union of Basic and Clinical Pharmacology. LXXIII. Nomenclature for the formyl peptide receptor (FPR) family. *Pharmacol Rev* 61(2):119–161.
12. Dufton N, et al. (2010) Anti-inflammatory role of the murine formyl-peptide receptor 2: Ligand-specific effects on leukocyte responses and experimental inflammation. *J Immunol* 184(5):2611–2619.
13. Brancaleone V, et al. (2013) A vasculo-protective circuit centered on lipoxin A4 and aspirin-triggered 15-epi-lipoxin A4 operative in murine microcirculation. *Blood* 122(4):608–617.
14. Brancaleone V, et al. (2011) Evidence for an anti-inflammatory loop centered on polymorphonuclear leukocyte formyl peptide receptor 2/lipoxin A4 receptor and operative in the inflamed microvasculature. *J Immunol* 186(8):4905–4914.
15. Cooray SN, et al. (2013) Ligand-specific conformational change of the G-protein-coupled receptor ALX/FPR2 determines proresolving functional responses. *Proc Natl Acad Sci USA* 110(45):18232–18237.
16. Cohen J (2002) The immunopathogenesis of sepsis. *Nature* 420(6917):885–891.
17. Scannell M, et al. (2007) Annexin-1 and peptide derivatives are released by apoptotic cells and stimulate phagocytosis of apoptotic neutrophils by macrophages. *J Immunol* 178(7):4595–4605.
18. Dalli J, et al. (2013) Proresolving and tissue-protective actions of annexin A1-based cleavage-resistant peptides are mediated by formyl peptide receptor 2/lipoxin A4 receptor. *J Immunol* 190(12):6478–6487.
19. Bone RC, et al.; The ACCP/SCCM Consensus Conference Committee; American College of Chest Physicians/Society of Critical Care Medicine (1992) Definitions for sepsis and organ failure and guidelines for the use of innovative therapies in sepsis. *Chest* 101(6):1644–1655.
20. Bone RC, et al. (1987) A controlled clinical trial of high-dose methylprednisolone in the treatment of severe sepsis and septic shock. *N Engl J Med* 317(11):653–658.
21. Ziegler EJ, et al. (1991) Treatment of gram-negative bacteremia and septic shock with HA-1A human monoclonal antibody against endotoxin. A randomized, double-blind, placebo-controlled trial. The HA-1A Sepsis Study Group. *N Engl J Med* 324(7):429–436.
22. Fisher CJ, Jr, et al.; The Soluble TNF Receptor Sepsis Study Group (1996) Treatment of septic shock with the tumor necrosis factor receptor:Fc fusion protein. *N Engl J Med* 334(26):1697–1702.
23. Fisher CJ, Jr, et al.; IL-1RA Sepsis Syndrome Study Group (1994) Initial evaluation of human recombinant interleukin-1 receptor antagonist in the treatment of sepsis syndrome: A randomized, open-label, placebo-controlled multicenter trial. *Crit Care Med* 22(1):12–21.
24. Dejager L, Pinheiro I, Dejonckheere E, Libert C (2011) Cecal ligation and puncture: The gold standard model for polymicrobial sepsis? *Trends Microbiol* 19(4):198–208.
25. Rivers E, et al.; Early Goal-Directed Therapy Collaborative Group (2001) Early goal-directed therapy in the treatment of severe sepsis and septic shock. *N Engl J Med* 345(19):1368–1377.
26. Coldewey SM, Rogazzo M, Collino M, Patel NS, Thiemermann C (2013) Inhibition of IκB kinase reduces the multiple organ dysfunction caused by sepsis in the mouse. *Dis Model Mech* 6(4):1031–1042.
27. Coldewey SM, et al. (2013) Erythropoietin attenuates acute kidney dysfunction in murine experimental sepsis by activation of the β-common receptor. *Kidney Int* 84(3):482–490.
28. Chen F, et al. (2014) Resolvin D1 improves survival in experimental sepsis through reducing bacterial load and preventing excessive activation of inflammatory response. *Eur J Clin Microbiol Infect Dis* 33(3):457–464.
29. Fullerton JN, O'Brien AJ, Gilroy DW (2013) Pathways mediating resolution of inflammation: When enough is too much. *J Pathol* 231(1):8–20.
30. Maddox JF, Serhan CN (1996) Lipoxin A$_4$ and B$_4$ are potent stimuli for human monocyte migration and adhesion: Selective inactivation by dehydrogenation and reduction. *J Exp Med* 183(1):137–146.
31. Wantha S, et al. (2013) Neutrophil-derived cathelicidin promotes adhesion of classical monocytes. *Circ Res* 112(5):792–801.
32. Yona S, et al. (2006) Impaired phagocytic mechanism in annexin 1 null macrophages. *Br J Pharmacol* 148(4):469–477.
33. Filep JG (2013) Biasing the lipoxin A4/formyl peptide receptor 2 pushes inflammatory resolution. *Proc Natl Acad Sci USA* 110(45):18033–18034.
34. Maderna P, et al. (2010) FPR2/ALX receptor expression and internalization are critical for lipoxin A$_4$ and annexin-derived peptide-stimulated phagocytosis. *FASEB J* 24(11):4240–4249.
35. Rudiger A, Singer M (2007) Mechanisms of sepsis-induced cardiac dysfunction. *Crit Care Med* 35(6):1599–1608.
36. Landry DW, Oliver JA (2001) The pathogenesis of vasodilatory shock. *N Engl J Med* 345(8):588–595.
37. Osuchowski MF, Welch K, Siddiqui J, Remick DG (2006) Circulating cytokine/inhibitor profiles reshape the understanding of the SIRS/CARS continuum in sepsis and predict mortality. *J Immunol* 177(3):1967–1974.
38. Khadour FH, et al. (2002) Enhanced NO and superoxide generation in dysfunctional hearts from endotoxemic rats. *Am J Physiol Heart Circ Physiol* 283(3):H1108–H1115.
39. Barth E, et al. (2006) Role of inducible nitric oxide synthase in the reduced responsiveness of the myocardium to catecholamines in a hyperdynamic, murine model of septic shock. *Crit Care Med* 34(2):307–313.
40. Mayadas TN, Cullere X, Lowell CA (2014) The multifaceted functions of neutrophils. *Annu Rev Pathol* 9:181–218.
41. Serhan CN, Savill J (2005) Resolution of inflammation: The beginning programs the end. *Nat Immunol* 6(12):1191–1197.
42. O'Hara R, Murphy EP, Whitehead AS, FitzGerald O, Bresnihan B (2004) Local expression of the serum amyloid A and formyl peptide receptor-like 1 genes in synovial tissue is associated with matrix metalloproteinase production in patients with inflammatory arthritis. *Arthritis Rheum* 50(6):1788–1799.
43. Iribarren P, et al. (2007) Interleukin 10 and TNFalpha synergistically enhance the expression of the G protein-coupled formylpeptide receptor 2 in microglia. *Neurobiol Dis* 27(1):90–98.
44. Ritchie RH, Gordon JM, Woodman OL, Cao AH, Dusting GJ (2005) Annexin-1 peptide Anx-1(2-26) protects adult rat cardiac myocytes from cellular injury induced by simulated ischaemia. *Br J Pharmacol* 145(4):495–502.
45. Ritchie RH, Sun X, Bilszta JL, Gulluyan LM, Dusting GJ (2003) Cardioprotective actions of an N-terminal fragment of annexin-1 in rat myocardium in vitro. *Eur J Pharmacol* 461(2-3):171–179.
46. Kim SD, et al. (2010) The agonists of formyl peptide receptors prevent development of severe sepsis after microbial infection. *J Immunol* 185(7):4302–4310.
47. Norling LV, Perretti M (2013) Control of myeloid cell trafficking in resolution. *J Innate Immun* 5(4):367–376.
48. Kapoor A, et al. (2010) Protective role of peroxisome proliferator-activated receptor-β/δ in septic shock. *Am J Respir Crit Care Med* 182(12):1506–1515.
49. Le Faouder P, et al. (2013) LC-MS/MS method for rapid and concomitant quantification of pro-inflammatory and pro-resolving polyunsaturated fatty acid metabolites. *J Chromatogr B Analyt Technol Biomed Life Sci* 932:123–133.
50. Perretti M, Solito E, Parente L (1992) Evidence that endogenous interleukin-1 is involved in leukocyte migration in acute experimental inflammation in rats and mice. *Agents Actions* 35(1-2):71–78.

Supporting Information

Gobbetti et al. 10.1073/pnas.1410938111

SI Methods

Animals. Male C57BL/6 or Fpr2/3$^{GFP/GFP}$ (thereafter referred to as Fpr2/3$^{-/-}$) mice, bearing a knocked-in gene for green fluorescent protein (1), were maintained on a standard chow pellet diet with free access to water and a 12-h light–dark cycle. All animal experiments were approved by the local Animal Use and Care Committee in accordance with the United Kingdom Animals (Scientific Procedures) Act of 1986. Human cells were prepared according to an approved protocol (East London & the City Local Research Ethics Committee; no. 06/Q605/40; P/00/029).

In Vivo Models.

Polymicrobial sepsis. Coecal ligature and puncture (CLP) was performed in 8-mo-old male C57BL/6 or Fpr2/3$^{-/-}$ mice using our published protocol that mimics clinical management in intensive care units (2), including fluid resuscitation (Acetated Ringer's solution; 0.5 mL per mouse), antibiotic therapy (Imipenem/Cilastin; 20 mg/kg body weight s.c.), and analgesia (buprenorphine; 0.05 mg/kg body weight i.p.) at 6 h and 18 h after surgery (2). In some experiments, mice were treated 1 and 9 h after CLP with a stable AnxA1-derived peptide, termed CR-AnxA1$_{2–50}$ (3 μg per mouse i.p.), or vehicle (saline/0.01% DMSO). Sham-operated mice underwent the same procedure but without CLP.

A clinical score for monitoring the health of experimental mice was used to evaluate the symptoms consistent with murine sepsis. The maximum score of 6 comprised the presence of the following signs: lethargy, piloerection, tremors, periorbital exudates, respiratory distress, and diarrhea. Mice with a clinical score >3 were defined as exhibiting severe sepsis, against a moderate sepsis for a score ≤3. Mice were killed 12 or 24 h later after assessment of cardiac function by echocardiography. Blood was collected by cardiac puncture and peritoneal lavage fluid, and kidney and lung tissue were also collected and stored at −80 °C for further analysis. Plasma and peritoneal cytokine levels were determined by cytokine beads assay (eBioscience). Peritoneal cells were counted using Turks solution and differentiated by flow cytometric analysis, as described below. Plasma was analyzed for levels of serum creatinine, urea, aspartate aminotransferase, and alanine transaminase (IDEXX Laboratories) for analysis.

Neutrophil phagocytosis and killing assay. Exudate neutrophils, obtained 6 h after i.p. injection of zymosan (3), were plated in 96-well plates at a density of 0.5×10^6 cells per well in complete medium. pH-sensitive Phrodo *E. coli* bioparticles (Invitrogen) were added to the cells. Neutrophils were labeled with anti-Ly6G, and the number of phagocytosing cells was measured by flow cytometry.

Neutrophil bactericidal activity was measured by incubating 2×10^6 neutrophils with 2×10^7 opsonized *E. coli* for 1 h. After infection, gentamicin (5 μg/mL) was added to the plates for 1 h, allowing the antibiotic to kill all bacteria that were not able to penetrate the cells and remained outside. The wells were then washed to remove the dead bacteria. Next the neutrophils were lysed using 0.1%Triton X-100, releasing the bacteria that penetrated the cells and remained alive. Lysates were then plated on solid medium plates, and the number or viable bacteria was determined by colony counting of live bacteria.

Bacteria counting. Accurate enumeration of bacteria in peritoneal lavages was performed by flow cytometry using the SYTO BC bacteria counting kit (Invitrogen) according to the manufacturer's instructions. Blood and peritoneal bacteria loads were also determined by growth on tryptic soy agar plate as reported previously (4).

Assessment of cardiac function in vivo (echocardiography). Cardiac function was assessed in mice by echocardiography in vivo as reported previously (5). At 24 h after CLP, anesthesia was induced with 3% (vol/vol) isoflurane and maintained at 0.5–1% for the duration of the procedure. Before assessment of cardiac function, mice were allowed to stabilize for at least 10 min. 2D and M-mode echocardiography images were recorded using a Vevo-770 imaging system (VisualSonics). Percentage fractional area change was assessed with a 2D trace of left ventricle (LV) and was derived by 100 × (LV end-diastolic area – LV end-systolic area) / LV end-diastolic area. The method involves tracing the endocardial surface of the LV in the parasternal short axis view at the level of papillary muscles. Percentage ejection fraction (EF) and percentage fractional shortening (FS) were calculated from the M-mode measurements of the LV internal dimension (LVID) in the diastolic (d) and systolic (d) phase, in the parasternal short axis view at the level of the papillary muscles. Percentage EF was calculated using the formula: $100 \times \{[\text{LVID (d)}^3 - \text{LVID (s)}^3] / \text{LVID (d)}^3\}$; percentage FS was derived using the formula: $100 \times \{[\text{LVID (d)} - \text{LVID (s)}] / \text{LVID (d)}\}$ (2, 5, 6).

Primary Macrophage and Human Monocyte Cultures. Mice were injected with 1 mL of 2% Bio-Gel (Bio-Rad) i.p., and 4 d later, peritoneal lavages were harvested with 4 mL of EDTA (3 mM) in PBS. Cells (0.5×10^6) were plated in 24-well plates in RPMI medium 1640 containing 10% (vol/vol) FCS and 50 mg/mL of gentamicin. After 2 h at 37 °C, nonadherent cells were washed and adherent cells (>90% macrophages) were incubated in RPMI 1640 1% FCS supplemented with specific cytokines (all at 50 ng/mL)—as indicated later—or vehicle. Cytokines were purchased from PeproTech. In a set of experiments, TNFα type I receptor null cells (from the colony described in ref. 7) were prepared and compared with macrophages prepared from C57BL/6 mice.

Primary human monocytes were extracted from the whole blood of healthy donors using the RosetteSep negative selection assay (Stem Cell Technologies Inc.) according to the manufacturer's protocols. Cells were resuspended in RPMI medium 1640, supplemented with 0.1% BSA, 100 U/mL penicillin, and 100 μg/mL streptomycin for all assays. Extractions were performed immediately before use in experiments.

Immunofluorescence Analyses. Peritoneal cells were fixed by incubation with 2% formaldehyde for 15 min at room temperature, washed, and immunostained for the monocyte/macrophage marker protein Iba1. Briefly, after 30 min at room temperature in 10% normal goat serum containing 0.025% saponin, cells were incubated for 1 h with a rabbit anti-mouse Iba1 polyclonal antibody (1/1,000; Wako Chemicals). After washing, cells were incubated for 30 min with AF594-conjugated goat anti-rabbit IgG secondary antibody (1/300), before further washing and mounting under glass coverslips using Moviol mounting agent (Sigma-Aldrich). Cells were then examined at 20× magnification using EVOS microscope (Life Technologies).

Biochemical Analyses.

Flow cytometry. Peritoneal cells were differentiated using anti-F4/80 (clone BM8; BioLegend), anti-Ly6G (clone 1A8; BioLegend), anti-CD3 (clone 145–2C11; eBioscience), and anti-B220 (clone

RA-3–6B2; BioLegend) antibodies. Fpr2/3 gene promoter activity was quantified by the proxy marker GFP (1). Isolated human monocytes were fixed with 2% (wt/vol) formaldehyde in 0.1 M of PBS before immunostaining with mouse monoclonal anti-FPR2 (Genovac), followed by secondary labeling with AF488-conjugated goat anti-mouse IgG (Invitrogen). In all cases, 20,000 events were acquired with a FACSCalibur (Becton Dickinson) and analyzed using FlowJo analysis software (version 9.2, Treestar Inc.).

Annexin A1 ELISA. Quantification of Annexin A1 in peritoneal lavages was obtained by sandwich ELISA as previously described (8).

Peritoneal lavage lipid quantification. Quantification of 6kPGF$_{1\alpha}$, TXB$_2$, PGE$_2$, LxA$_4$, LTB$_4$, and PGD$_2$ in peritoneal lavages was achieved by LC–MS/MS measurements as described (9, 10). Briefly, to simultaneously separate lipids of interest and three deuterated internal standards, LC–MS/MS analysis was performed on the UHPLC (ultra high performance liquid chromatography) System (Agilent LC1290 Infinity) coupled to Agilent 6460 triple quadruple MS (Agilent Technologies) equipped with electrospray ionization operating in negative mode. Reverse-phase UHPLC was performed using ZorBAX SB-C18 column (2.1 mm, 50 mm, 1.8 μm) (Agilent Technologies) with a gradient elution. Data were acquired in Multiple Reaction Monitoring mode with optimized conditions (ion optics and collision energy). Peak detection, integration, and quantitative analysis were done using Mass Hunter Quantitative analysis software (Agilent Technologies). For each standard, calibration curves were built using 10 solutions at concentrations ranging from 0.95 ng/mL to 500 ng/mL.

Determination of MPO activity in heart, kidney, and lung tissue. Myeloperoxidase (MPO) activity was measured as an index of blood-borne PMN infiltration as described (11).

Real-time PCR analysis. Total RNA from biogel-elicited macrophages was isolated with TRIzol reagent (Invitrogen) according to the manufacturer's protocol. In all cases, total RNA (1 μg) was reverse-transcribed with random hexamer oligonucleotides and SuperScript III (Invitrogen). Amplification was performed with a LightCycler 480 using a SYBR Green I Master Kit (Qiagen Ltd.) and the mouse Fpr2 primer set (QT00171514, Qiagen). Relative expression of the target gene was normalized to expression of the Hypoxanthine Phosphoribosyltransferase (*Hprt*) gene, using the $\Delta\Delta C_t$ method.

Statistical Analyses. Sepsis clinical score analysis was performed using Fisher's exact test (2 × 2 tables). Statistical differences were determined using one- or two-way analysis of variance, as appropriate, followed by Tukey's posttest. A P value < 0.05 was taken as significant for rejection of the null hypothesis.

1. Dufton N, et al. (2010) Anti-inflammatory role of the murine formyl-peptide receptor 2: Ligand-specific effects on leukocyte responses and experimental inflammation. *J Immunol* 184(5):2611–2619.
2. Coldewey SM, et al. (2013) Erythropoietin attenuates acute kidney dysfunction in murine experimental sepsis by activation of the β-common receptor. *Kidney Int* 84(3):482–490.
3. Perretti M, Solito E, Parente L (1992) Evidence that endogenous interleukin-1 is involved in leukocyte migration in acute experimental inflammation in rats and mice. *Agents Actions* 35(1-2):71–78.
4. Spite M, et al. (2009) Resolvin D2 is a potent regulator of leukocytes and controls microbial sepsis. *Nature* 461(7268):1287–1291.
5. Kapoor A, et al. (2010) Protective role of peroxisome proliferator-activated receptor-β/δ in septic shock. *Am J Respir Crit Care Med* 182(12):1506–1515.
6. Khan AI, et al. (2013) Erythropoietin attenuates cardiac dysfunction in experimental sepsis in mice via activation of the β-common receptor. *Dis Model Mech* 6(4): 1021–1030.
7. Rothe J, et al. (1993) Mice lacking the tumour necrosis factor receptor 1 are resistant to TNF-mediated toxicity but highly susceptible to infection by Listeria monocytogenes. *Nature* 364(6440):798–802.
8. McArthur S, et al. (2010) Annexin A1: A central player in the anti-inflammatory and neuroprotective role of microglia. *J Immunol* 185(10):6317–6328.
9. Gobbetti T, et al. (2013) Polyunsaturated fatty acid metabolism signature in ischemia differs from reperfusion in mouse intestine. *PLoS ONE* 8(9):e75581.
10. Le Faouder P, et al. (2013) LC-MS/MS method for rapid and concomitant quantification of pro-inflammatory and pro-resolving polyunsaturated fatty acid metabolites. *J Chromatogr B Analyt Technol Biomed Life Sci* 932:123–133.
11. Gobbetti T, et al. (2012) Serine protease inhibition reduces post-ischemic granulocyte recruitment in mouse intestine. *Am J Pathol* 180(1):141–152.

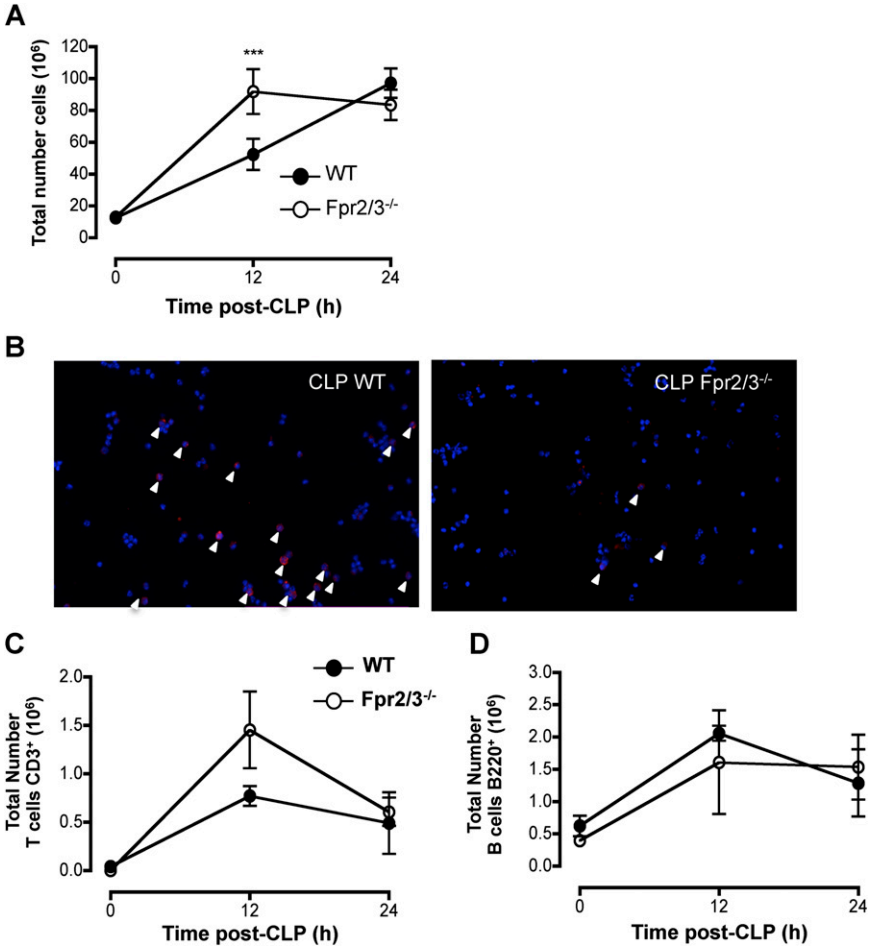

Fig. S1. Cell phenotype during ongoing CLP. WT and Fpr2/3$^{-/-}$ mice were subjected to CLP at time 0 (*Methods*). (*A*) Temporal changes in total number of cells recruited in the peritoneal cavity post-CLP in WT and Fpr2/3$^{-/-}$ animals. Data are mean ± SEM of six mice per genotype. ***$P < 0.001$ versus respective WT value (two-way ANOVA, post hoc Tukey test). (*B*) Immunofluorescent microscopic analysis of Iba1-positive cells (arrowheads) in peritoneal exudates 24 h post-CLP from WT and Fpr2/3$^{-/-}$ mice. (*C* and *D*) Cumulative data for CD3^{+} (T cells) and B220^{+} (B cells) in the peritoneal cavity post-CLP from WT and Fpr2/3$^{-/-}$ mice. Data are mean ± SEM of six mice per genotype.

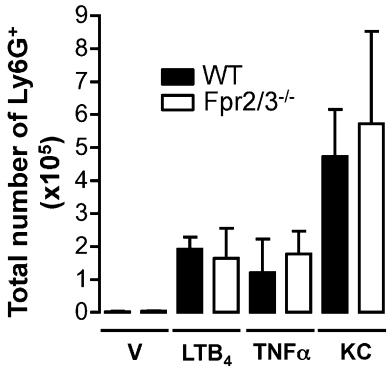

Fig. S2. Fpr2/3 deficiency does not affect neutrophil recruitment for classical chemoattractants. Mice were injected i.p. with three classical neutrophil chemoattractants (LTB4, 100 ng; TNFa, 1 μg; KC, 1 μg) or vehicle (V; 100 μL). Four hours after the injection, peritoneal lavages were collected. Cells were stained for Ly6G or F4/80. Data are mean ± SEM of 4–5 mice per group.

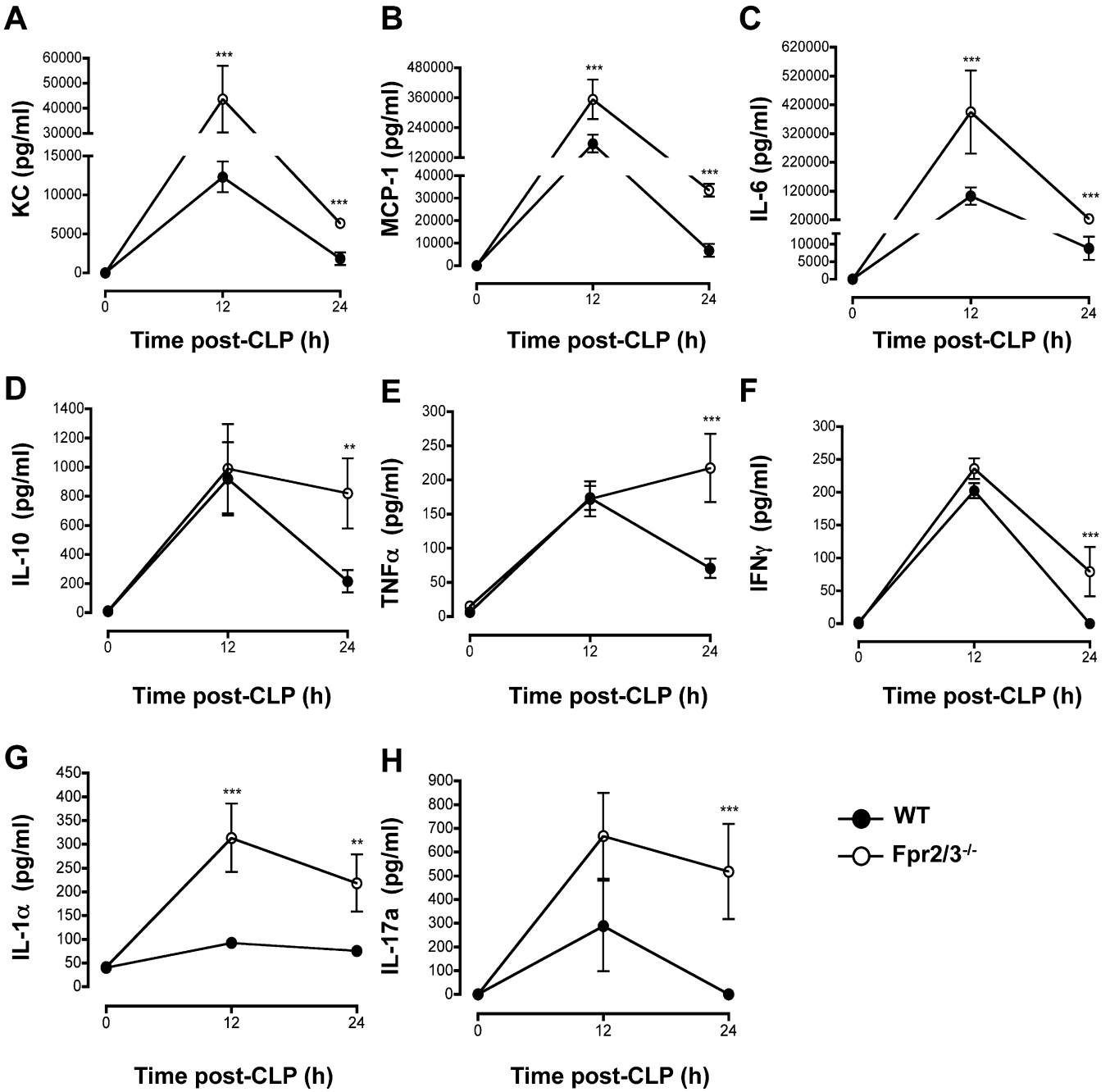

Fig. S3. Peritoneal soluble inflammatory mediator generation in Fpr2/3$^{-/-}$ mice during polymicrobial sepsis. WT and Fpr2/3$^{-/-}$ mice were subjected to CLP at time 0 (*Methods*). (*A–H*) At 24 h post-CLP, blood was collected and plasma samples prepared and tested for cytokine levels using the cytokine bead assay by flow cytometry. Data are mean ± SEM of six mice per group. $^{**}P < 0.01$, $^{***}P < 0.001$ versus correspondent WT value (two-way ANOVA, post hoc Tukey test).

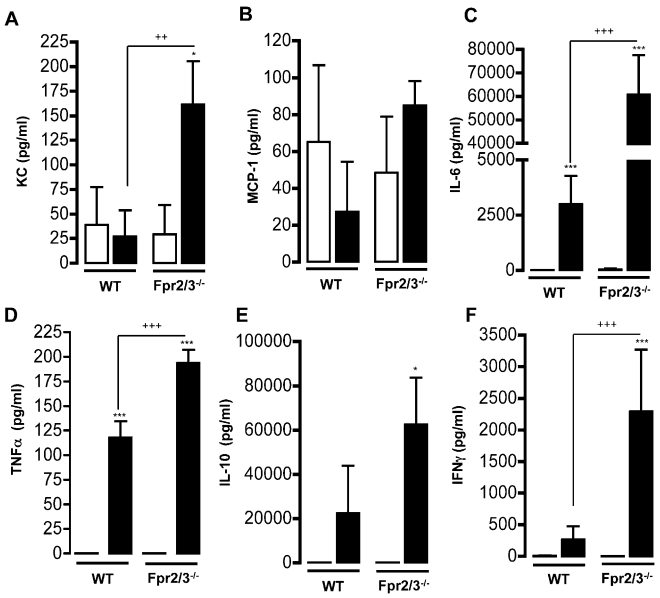

Fig. S4. Plasma soluble inflammatory mediator generation in Fpr2/3$^{-/-}$ mice during polymicrobial sepsis. WT and Fpr2/3$^{-/-}$ mice were subjected to CLP at time 0 (*Methods*). (*A–F*) At 24 h post-CLP, blood was collected and plasma samples prepared and tested for cytokine levels using the cytokine bead assay by flow cytometry. Data are mean ± SEM of six mice per group. $^{**}P < 0.01$, $^{***}P < 0.001$ versus correspondent WT value (two-way ANOVA, post hoc Tukey test).

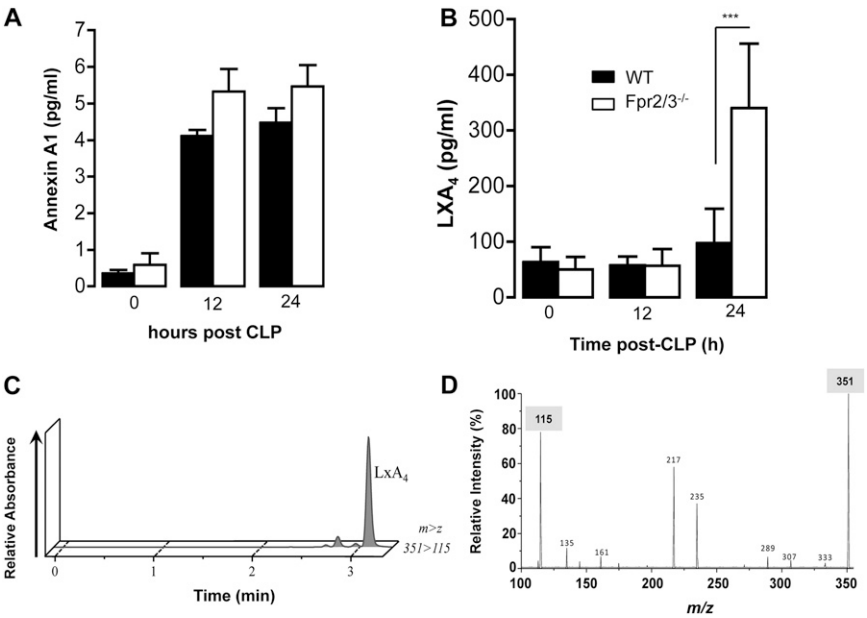

Fig. S5. Annexin A1 and Lipoxin A_4 levels in peritoneal exudates during polymicrobial sepsis. WT and Fpr2/3$^{-/-}$ mice were subjected to CLP at time 0 (*Methods*). (*A*) Annexin A1 was quantified by sandwich ELISA. Quantitative Annexin A1 levels over the time course of the CLP response. (*B*) Lipoxin A_4 (LXA_4) was identified and quantified by LC–MS/MS-based lipidomic analysis. Quantitative LXA_4 levels over the time course of the CLP response. (*C*) Spectrum of relative peaks for LXA_4. (*D*) LXA_4 signature fragment ions reported as *m/z*, highlighting the two diagnostic fragments at 115 and 351 (351 is the ion mass). Data are mean ± SEM of six mice. $^{***}P < 0.001$ versus correspondent WT value (two-way ANOVA, post hoc Tukey test).

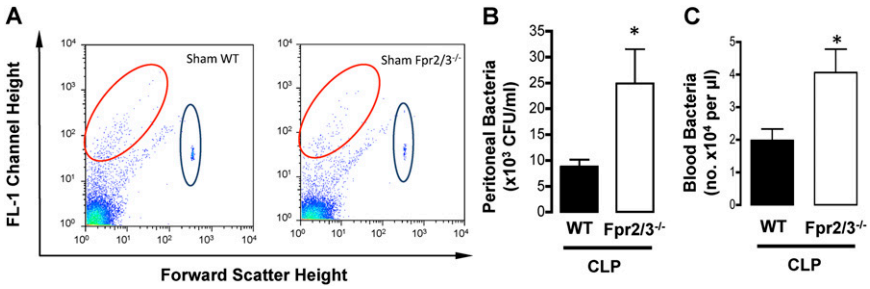

Fig. S6. Sham settings and bacterial levels in CLP. WT and Fpr2/3$^{-/-}$ mice were subjected to CLP at time 0 (*Methods*). (*A*) Representative flow cytometry scattergrams illustrating bacteria (SYTO BC bacteria dye) positive events in sham peritoneal exudates from WT (*Left*) and Fpr2/3$^{-/-}$ (*Right*) mice. The density of bacteria in the experimental samples was determined from the ratio of bacterial to microsphere signals. (*B*) Measurement of aerobic bacteria levels in peritoneal lavages 24 h post-CLP from WT and Fpr2/3$^{-/-}$ mice. Data are mean ± SEM of six mice. *$P < 0.05$ versus correspondent WT value (Student *t* test). (*C*) Measurement of bacterial levels 24 h after CLP in plasma from WT and Fpr2/3$^{-/-}$ mice. Data are mean ± SEM of six mice. *$P < 0.05$ versus correspondent WT value (Student *t* test).

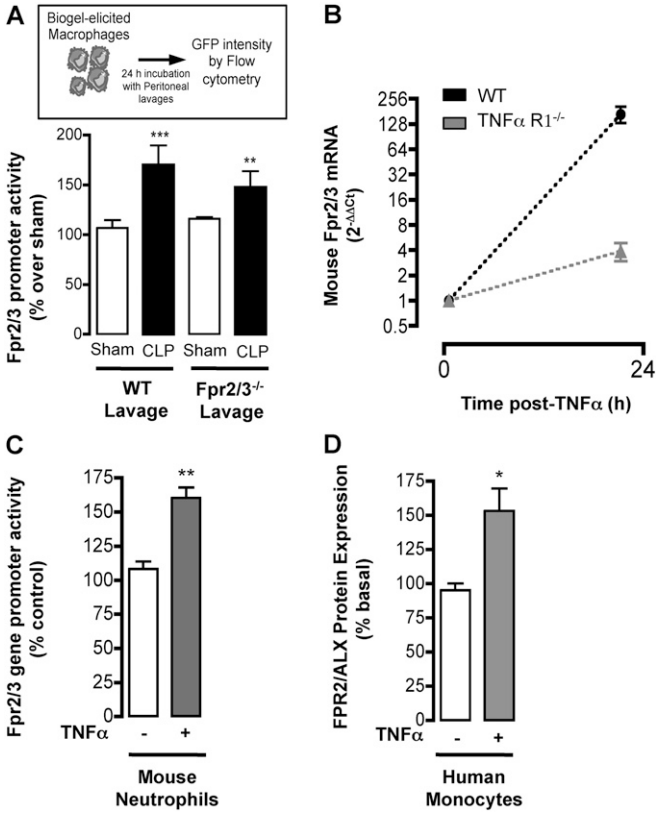

Fig. S7. Fpr2 modulation in mouse and human cells. (*A*) Biogel-elicited macrophages from Fpr2/3$^{-/-}$ mice were incubated with sham or 24-h CLP lavages (collected from WT or Fpr2/3$^{-/-}$ animals) for 24 h at 37 °C, before assessment of GFP fluorescence by flow cytometry. Data are mean ± SEM of six mice per group. **$P < 0.01$, ***$P < 0.001$ versus correspondent sham value (two-way ANOVA, post hoc Tukey test). (*B*) Biogel-elicited macrophages from WT and TNFαR1$^{-/-}$ mice were incubated for 24 h with 50 ng/mL TNFα before Fpr2/3 mRNA quantification by real-time PCR. Data are mean ± SEM of 4–6 distinct cell preparations. ***$P < 0.001$ versus WT value (two-way ANOVA, post hoc Tukey test). (*C*) Zymosan-elicited PMN from Fpr2/3$^{-/-}$ mice were incubated for 24 h with 50 ng/mL TNFα before assessment of GFP fluorescence by flow cytometry, used as a reporter for Fpr2/3 gene promoter activity. (*D*) Human monocytes were incubated for 24 h with 50 ng/mL TNFα before assessment of FPR2/ALX expression by flow cytometry. Data are mean ± SEM of 3–4 distinct cell preparations. *$P < 0.05$, **$P < 0.01$ versus control (Student *t* test).

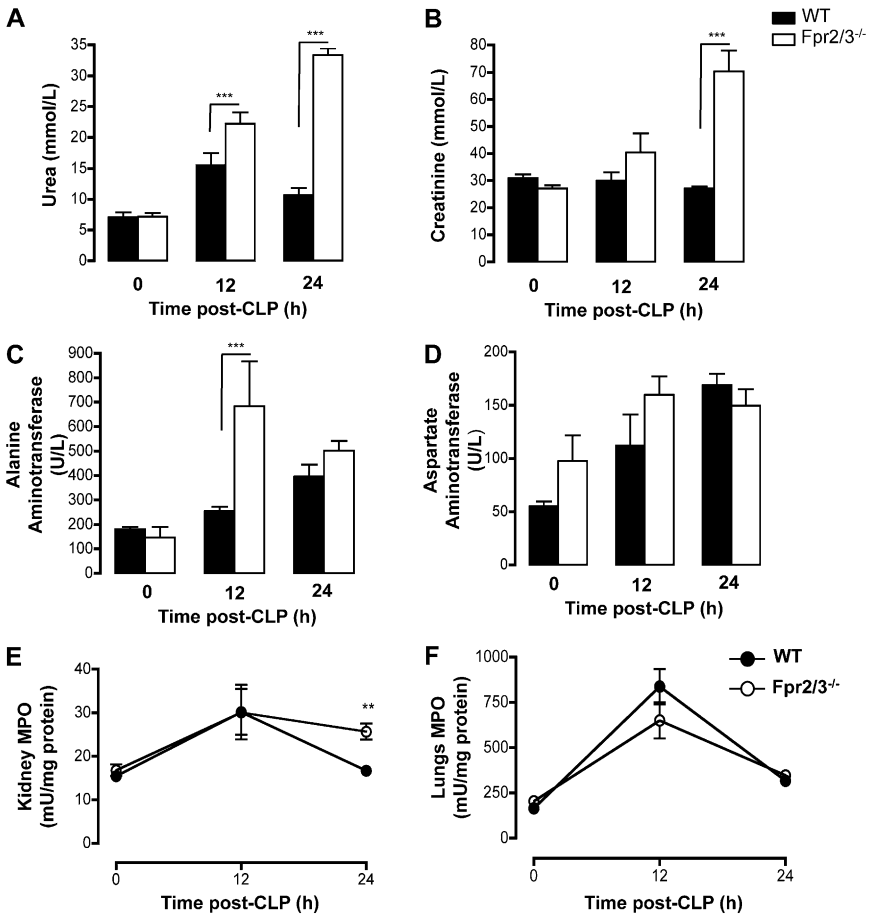

Fig. S8. Organ injury modulation between the two genotypes. WT and Fpr2/3$^{-/-}$ mice were subjected to CLP at time 0 (*Methods*). (*A* and *B*) Temporal changes in plasma urea and creatinine post-CLP in WT and Fpr2/3$^{-/-}$ animals. (*C* and *D*) Temporal changes in plasma alanine aminotransferase and aspartate aminotransferase post-CLP in WT and Fpr2/3$^{-/-}$ animals. (*E* and *F*) Kidney and lung MPO activity at different times post-CLP. Data are mean ± SEM of six mice. $^{**}P < 0.01$, $^{***}P < 0.001$ between genotypes (two-way ANOVA, post hoc Tukey test).

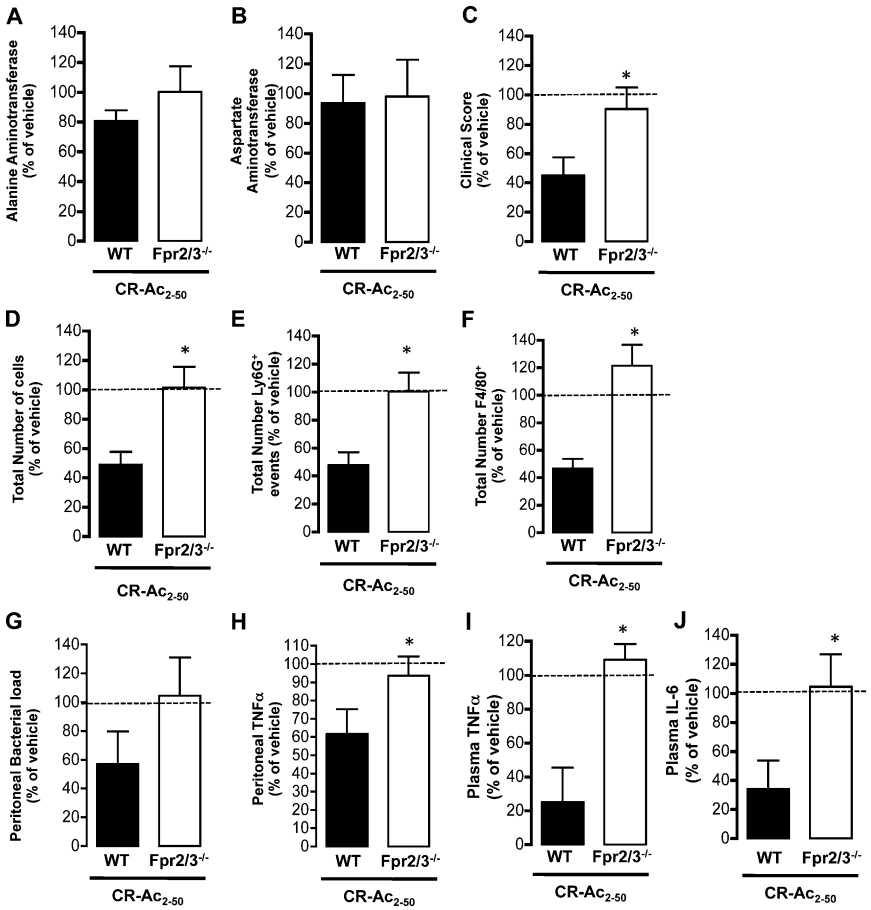

Fig. S9. Fpr2/3 agonism modulates the host response to polymicrobial sepsis. WT and Fpr2/3$^{-/-}$ mice were subjected to CLP at time 0 (*Methods*) and treated with an AnxA1-based peptide CR-Ac$_{2-50}$ 1 h and 9 h postsurgery, using a dose of 90 μg/kg i.p., or with vehicle (100 μL i.p.), and killed at 24 h post-CLP. (*A* and *B*) Plasma alanine aminotransferase and aspartate aminotransferase values in WT and Fpr2/3$^{-/-}$ animals. (*C*) Presence or absence of six different macroscopic signs of sepsis—namely, lethargy, piloerection, tremors, periorbital exudates, respiratory distress, and diarrhea. (*D–F*) Cumulative data for total number of cells, Ly6G+ cells (neutrophils), and monocyte–macrophage (F4/80+ cells; Mo) counts in peritoneal exudates from WT and Fpr2/3$^{-/-}$ mice treated i.p. with vehicle or CR-Ac$_{2-50}$. (*G*) Peritoneal bacterial load. (*H*) CR-Ac$_{2-50}$ treatment reduces exudate TNFa, compared with vehicle, in WT but not Fpr2/3$^{-/-}$ mice. (*I* and *J*) CR-Ac$_{2-50}$ treatment reduces plasma TNFa and IL-6 levels, compared with vehicle, in WT but not Fpr2/3$^{-/-}$ mice. Data are mean ± SEM of six mice per group. *$P < 0.05$ versus correspondent WT value (Student *t* test).

Table S1. Bioactive lipid mediator quantification in peritoneal exudates

Genotype	Treatment	PGE_2, pg/mL	TXB_2, pg/mL	6-keto-$PGF_1\alpha$, pg/mL	LTB_4, pg/mL	PGD_2, pg/mL
WT	Sham	106 ± 8	62 ± 38	362 ± 85	30 ± 20	105 ± 7
	CLP 12 h	426 ± 148	439 ± 70	5,229 ± 1,365	210 ± 46	13 ± 13
	CLP 24 h	813 ± 258	628 ± 187	4,006 ± 11	348 ± 103	839 ± 401
Fpr2/3$^{-/-}$	Sham	126 ± 24	30 ± 25	346 ± 103	30 ± 18	120 ± 32
	CLP 12 h	1,026 ± 382	710 ± 161	10,616 ± 2,370*	630 ± 186	48 ± 39
	CLP 24 h	5,297 ± 2,257***	1,405 ± 493	20,628 ± 5,360**	746 ± 292	2,458 ± 1,015

WT and Fpr2/3$^{-/-}$ mice were subjected to CLP at time 0 (*Methods*), with sham animals being operated without cecum damage. Cell-free lavage fluids were analyzed by LC–MS/MS-based lipidomic analysis for multiple lipid mediators. Data (mean ± SEM of six mice per group) are expressed as concentrations. Results are mean ± SEM of six mice. *$P < 0.05$, **$P < 0.01$, ***$P < 0.001$ versus respective WT value (two-way ANOVA, post hoc Tukey test).